A thermodynamic method for the construction of a cohesive law from a nonlocal damage model

Fabien Cazes, Michel Coret, Alain Combescure, Anthony Gravouil

A thermodynamic method for the construction of a cohesive law from a nonlocal damage model

Fabien Cazes [a], Michel Coret [a], Alain Combescure [a], Anthony Gravouil [a] [a]

Université de Lyon, CNRS INSA-Lyon, LaMCoS UMR5259, F-69621, France

Several published papers deal with the possibility of replacing a damage finite element model by a combination of cohesive zones and finite elements. The focus of the paper is to show under which conditions this change of model can be done in an energy-wise manner.

The objective is to build a cohesive model based on a known damage model, without making any assumption on the shape of the cohesive law. The method is characterized, on the one hand, by the use of a well-defined thermodynamic framework for the cohesive model and, on the other hand, by the idea that the main quantity which must be maintained through the change of model is the energy dissipated by the structure. An analysis of the stability criteria enables us to determine the domains of validity of the different models. Thus, we show that it is consistent to derive the cohesive law from a given nonlocal damage model because the occurrence of a discontinuity can be viewed as an alternative way to limit localization. The method is illustrated on one-dimensional examples and a numerical resolution method for the problem with a cohesive zone is presented.

Keywords:
Fracture mechanics
Damage
Nonlocal models
Cohesive zone models

1. Introduction

The simulation of crack initiation and propagation has always been a difficult challenge, but it is always improving. In case of continuum mechanics for homogeneous medium, the finite element simulation of crack initiation is rather well understood. It involves two main ingredients: the damage theory, and the introduction of nonlocal modeling or second-gradient theory to avoid artificial localization. However, even if it is possible to predict crack propagation with this framework, this approach is not very robust and needs refined meshes along the whole (unknown) crack path to be predictive. Some authors have then avoided the use of critically damaged elements, by introducing cohesive segments, or elements which can inherit embedded discontinuities. The position and the direction of the initial cohesive segment are based on sound physical arguments: e.g. critical stress reached within the element, initial cohesive zone perpendicular to the direction of principal maximum tensile stress.

On the other hand, significant progress have been obtained in the simulation of crack propagation by the development of the X-FEM method (Belytschko and Black, 1999; Moes et al., 1999) which can be combined with the use of cohesive zone models Wells and Sluys, 2001; Moës and Belytschko, 2002; Mariani and Perego, 2003; Simone et al., 2003. This method is well adapted to the propagation of "long" cracks but not for the initiation phase, when cracks are short and singular functions describing the fields near the crack tip are not valid.

This paper is devoted to the following question: under which conditions is it possible to replace a fine model describing a localization process (using damage theory combined with nonlocal models) by a coarser mesh containing an explicit description of a discontinuity using cohesive zones combined or not with X-FEM? We show that it is possible to construct the cohesive law in such a way that the change of model is perfectly thermodynamically coherent: this implies that during this numerical change of model no energy, stored or dissipated, is artificially inserted or withdrawn between the two models. This point is crucial to be really predictive in this domain.

Rupture within a material is hard to model because the nature of the phenomena involved changes over time. Often, rupture begins with a global interaction of all the microscopic defects initially present until the coalescence of some of these defects results in the creation of a macroscopic crack in the material. Thus, there is a transition from microscopic, diffuse phenomena toward macroscopic, localized phenomena.

This complexity of the rupture process justifies the existence of two main families of models to represent the same phenomena: continuous damage models (Kachanov, 1958; Lemaitre and Chaboche, 1988), which follow a thermodynamic approach and are based on the concept of a representative elementary volume, and models in which a discontinuity is allowed to propagate within the structure, among which Griffith's model (Griffith, 1920) and

cohesive zone models (Barenblatt, 1962; Dugdale, 1960) deserve special mention.

The objective of this paper is to establish a coupling between these two visions of rupture based on energy criteria. Our starting point is the principle proposed in Mazars (1984) that the quantity which must be preserved in achieving this coupling between models is the dissipated energy (see also Mazars and Pijaudier-Cabot, 1996). Our preference goes toward the use of fracture models of the cohesive zone type because these are more capable of detecting crack initiation than Griffith's model (Charlotte et al., 2000). We finally derive a cohesive law given a damage model without making any assumption on the shape of the cohesive law. Even if fracture process usually dissipates energy by plastic deformation and frictional mechanisms during a closure, damage will be the only dissipative mechanism considered in this article for sake of simplicity.

We will see that the use of a nonlocal continuous model is necessary to model accurately a localized damaged state. Though the thermodynamic description of nonlocal models is not perfectly understood yet, it allows to take into account the complex mechanisms of micro-cracking that occur on a spatially extended zone for the construction of the cohesive zone model. Another interest of the method is that the shape of the cohesive law is not fixed in advance and only determined from the knowledge of the reference damage model. The obtained cohesive law can then be used independently of the underlying continuous model.

In the first section, we review some results from the thermodynamics of cohesive models, according to Gurtin (1979).

In the second section, we present the models which will be used in the rest of the work: an isotropic damage model and a cohesive model in which closing is assumed to be linear.

In the third section, we address the question of the validity of the proposed coupling, which must take place at the intersection of the domains of validity of the models being used. This point is far from trivial because, *a priori*, continuous models are better suited for the modeling of diffuse phenomena, whereas discontinuous models are better suited for the modeling of localized phenomena. This part of our study leads to the choice of a continuous model of the nonlocal damage type and of a discontinuous model which allows the formation of a cohesive zone in a damageable material.

In the fourth section, we present criteria for the coupling of these models. We show that by enforcing equal dissipated energies in the continuous and discontinuous models, using a cohesive model with linear closing under prescribed displacement boundary conditions, one can achieve the identification of each term of the energy balance of the coupled models. Thus, one ends up with truly equivalent models from an energy standpoint.

In the fifth section, we apply our proposed coupling method to the incremental determination of a cohesive law based on a nonlocal damage calculation. We first study the simplified case where localization is limited by assuming that damage is homogeneous within the beam, then move to the case of a true nonlocal damage model. A numerical method of resolution with a cohesive zone is proposed.

2. Thermodynamic construction of a cohesive model

2.1. Definition of the variables of the cohesive model

We consider a continuous media with a crack defined by a discontinuity surface. Let us choose a basis $\mathscr{B}_s$ defined by its unit vectors $(\underline{n}, \underline{t}_1, \underline{t}_2)$, where $\underline{n}$ is normal to the discontinuity Γ_s. $\underline{t}_1$ and $\underline{t}_2$ are chosen such that $\mathscr{B}_s$ is a direct orthogonal basis. This basis is defined according to the position of the crack in the undeformed configuration. The direction chosen for $\underline{n}$ permits to define the upper and lower lips Γ_s^+ and Γ_s^- of the crack. Under the small perturbation assumption, let us define the displacement jump $[\![\underline{u}]\!]$ as the difference between the displacement fields $\underline{u}^+$ and $\underline{u}^-$ of the crack's upper and lower lips, respectively.

$$[\![\underline{u}]\!] = \underline{u}^+ - \underline{u}^- \quad \text{over } \Gamma_s. \tag{1}$$

The projection of the displacement jump $[\![\underline{u}]\!]$ onto $\mathscr{B}_s$ leads to the definition of $[\![u]\!]_n$, $[\![u]\!]_{t_1}$ and $[\![u]\!]_{t_2}$ such that

$$[\![\underline{u}]\!] = \begin{pmatrix} [\![u]\!]_n \\ [\![u]\!]_{t_1} \\ [\![u]\!]_{t_2} \end{pmatrix}_{\mathscr{B}_s}. \tag{2}$$

Let us consider the cohesive zone alone. The principle of virtual power, in statics, is expressed as

$$\mathscr{P}^*_{int}([\![\underline{u}]\!]^*) + \mathscr{P}^*_{ext}([\![\underline{u}]\!]^*) = 0 \quad \forall [\![\underline{u}]\!]^* \in \mathscr{C}, \tag{3}$$

where $\mathscr{P}^*_{int}$ is the virtual power of the internal loads, $\mathscr{P}^*_{ext}$ the virtual power of the external loads and $\mathscr{C}$ a field of continuous, regular and kinematically admissible vectors defined over Γ_s. The vector of the cohesive stresses $\underline{\sigma}^s$ is defined by

$$\mathscr{P}^*_{int} = -\int_{\Gamma_s} \underline{\sigma}^s \frac{d[\![\underline{u}]\!]^*}{dt} dS. \tag{4}$$

$[\![\underline{u}]\!]^*$ is a virtual displacement jump and t is the time. Let σ^s, τ_1^s and τ_2^s designate the components of $\underline{\sigma}^s$ in $\mathscr{B}_s$:

$$\underline{\sigma}^s = \begin{pmatrix} \sigma^s \\ \tau_1^s \\ \tau_2^s \end{pmatrix}_{\mathscr{B}_s}. \tag{5}$$

Under the small perturbation assumption, integration can be carried out equally well on the Eulerian or Lagrangian configuration. Thus, $\int_{\Gamma_s^+} = \int_{\Gamma_s^-} = \int_{\Gamma_s}$. Then, the virtual power of the external loads has the following expression:

$$\mathscr{P}^*_{ext} = \int_{\Gamma_s} \left(\underline{\underline{\sigma}}^+ \underline{n} \frac{d(\underline{u}^+)^*}{dt} - \underline{\underline{\sigma}}^- \underline{n} \frac{d(\underline{u}^-)^*}{dt} \right) dS \tag{6}$$

with $\underline{\underline{\sigma}}^-$ being the stress tensor along the crack's lower lip and $\underline{\underline{\sigma}}^+$ being the stress tensor along the crack's upper lip.

By choosing the proper virtual fields, one obtains the equilibrium equations of the structure in the cohesive zone:

$$\underline{\sigma}^s = \underline{\underline{\sigma}}^+ \underline{n} = \underline{\underline{\sigma}}^- \underline{n} \quad \text{over } \Gamma_s. \tag{7}$$

2.2. Application of the principles of thermodynamics to the cohesive zone

Let us define the heat flow jump $[\![\underline{q}]\!]$ as

$$[\![\underline{q}]\!] = (\underline{q}^+ - \underline{q}^-)\underline{n}. \tag{8}$$

One can show (Gurtin, 1979) that the local expressions of the first and second principles at a point of the discontinuity Γ_s are

$$\frac{de_s}{dt} = \underline{\sigma}^s \frac{d[\![\underline{u}]\!]}{dt} + [\![\underline{q}]\!]\underline{n}, \tag{9}$$

$$\frac{ds_s}{dt} = \frac{[\![\underline{q}]\!]\underline{n}}{T} + \frac{d(s_i)_s}{dt}. \tag{10}$$

e_s being the surface density of internal energy, s_s the surface density of entropy, $(s_i)_s$ the surface density of internal entropy and $[\![\underline{u}]\!]$ the actual displacement jump. Multiplying this last expression by the temperature, one gets the dissipated surface energy of the cohesive zone (such that $d\phi_s = Td(s_i)_s$):

$$\frac{d\phi_s}{dt} = T\frac{ds_s}{dt} - [\![\underline{q}]\!]\underline{n}. \tag{11}$$

The free surface energy of the cohesive zone ψ_s is defined by

$$\psi_s = e_s - Ts_s. \tag{12}$$

Introducing (9) and (12) into (11), one gets the equivalent of the Clausius–Duhem inequality for the cohesive zone:

$$d\phi_s = \underline{\sigma}^s d[\![\underline{u}]\!] - d\psi_s - s_s dT \geqslant 0. \tag{13}$$

Let us note that there is no term associated with the temperature gradient across the discontinuity, which is anyway undefined over Γ_s. Therefore, there is no thermal dissipation associated with the cohesive zone, and ϕ_s can be considered to be equal to the intrinsic dissipated energy ϕ_s^1 of the cohesive zone:

$$\phi_s = \phi_s^1. \tag{14}$$

2.3. Thermodynamic potential

As in Costanzo and Allen (1995), we assume that the cohesive zone behaves like a standard generalized material. We also assume that there is no plasticity in the behavior of the cohesive zone and, therefore, that we do not need to define irreversible cohesive stresses. This is justified by the fact there is also no plasticity in the behavior of the damage model we intend to use as the reference model. Therefore, we use a free energy potential ψ_s which can be assumed to depend only on the displacement jump $[\![\underline{u}]\!]$, temperature T and on some internal variables denoted v_k.

$$\psi_s = \psi_s([\![\underline{u}]\!], T, v_k). \tag{15}$$

One can then show (Gurtin, 1979) that

$$\underline{\sigma}^s = \frac{\partial \psi_s}{\partial [\![\underline{u}]\!]} \quad \text{and} \quad s_s = -\frac{\partial \psi_s}{\partial T}. \tag{16}$$

Let us denote A_k the variables associated with the internal variables v_k, i.e.,

$$A_k = \frac{\partial \psi_s}{\partial v_k}, \tag{17}$$

which enables one to show that the increment of dissipated surface energy $d\phi_s$ is

$$d\phi_s = -A_k dv_k. \tag{18}$$

3. The energy framework and the models being considered

3.1. General expression of the total energy for a rupture problem

Now we are going to define an energy framework for the rupture process independently of the model chosen to study the phenomenon by considering the case of an isothermal transformation applied to an isolated volume denoted Ω. Let $\mathscr{E}$ be the total energy, defined as the energy quantity which remains constant over time. In order to obtain an expression of $\mathscr{E}$, we start from the local expressions of the dissipated energy given by the left-hand side of the Clausius–Duhem inequality in the isothermal case for a continuous model and for a discontinuous model (13):

$$d\phi = \underline{\underline{\sigma}} : d\underline{\underline{\varepsilon}} - \rho d\psi \quad \text{over } \Omega, \tag{19}$$

$$d\phi_s = \underline{\sigma}^s d[\![\underline{u}]\!] - d\psi_s \quad \text{over } \Gamma_s, \tag{20}$$

ϕ being the dissipated volume energy, ρ the mass density, ψ the free energy per unit mass, $\underline{\underline{\sigma}}$ the Cauchy stress tensor and $\underline{\underline{\varepsilon}}$ the linearized strain tensor. By integrating these expressions over Ω and Γ_s, one gets

$$d\Phi = -d\Psi - dW_{int}, \tag{21}$$

where Φ, Ψ and W_{int} represent the dissipated energy, the free energy and the work of the internal forces of the whole structure, respectively. Then, the application of the work–energy theorem leads to the following expression of the total energy:

$$\mathscr{E} = \Psi + K - W_{ext} + \Phi, \tag{22}$$

where K is the kinetic energy and W_{ext} the work of the external forces.

3.2. The damage model

The damage model (Kachanov, 1958; Lemaitre and Chaboche, 1988) is derived from the thermodynamics of continuous media. In the isothermal case, the free energy potential has the following expression:

$$\rho\psi = \frac{1}{2}(1-D)\ \underline{\underline{\varepsilon}} : \mathbf{K} : \underline{\underline{\varepsilon}}, \tag{23}$$

where D is the damage variable, $\underline{\underline{\varepsilon}}$ the linearized strain tensor and $\mathbf{K}$ the Hooke's tensor of the healthy material. The value of $\underline{\underline{\sigma}}$ calculated from ψ is

$$\underline{\underline{\sigma}} = \rho \frac{\partial \psi}{\partial \underline{\underline{\varepsilon}}} = (1-D)\mathbf{K} : \underline{\underline{\varepsilon}}. \tag{24}$$

Now, let us define a cohesive model consistent with this damage model used as the reference.

3.3. The cohesive model with linear closing

For the damage model, we know that the unloading behavior of the material is linear elastic. Therefore, the closing is nondissipative and the expression of the thermodynamic potential can be replaced by its second-order expansion. Since we are trying to couple the cohesive model with a damage model, it is natural to impose the same closing conditions on the cohesive model being used. Since we are dealing with the isothermal case, let us describe the behavior of the cohesive zone using a free energy potential defined in terms of the only observable variable $[\![\underline{u}]\!]$, plus some internal variables denoted v_k:

$$\psi_s = \psi_s([\![\underline{u}]\!], v_k). \tag{25}$$

The increment of dissipated energy can be calculated using Expression (18). Thus, an increase in the system's entropy affects only the evolution of the internal variables. Since the closing is nondissipative, we can consider that during a closing phase the thermodynamic potential depends on the observable variable alone:

$$\psi_s = \psi_s([\![\underline{u}]\!]). \tag{26}$$

Since the behavior during closing is linear, let us choose a potential ψ_s with a quadratic expression

$$\psi_s = \underline{\sigma}_0^s [\![\underline{u}]\!] + \frac{\eta}{2}[\![\underline{u}]\!]^2, \tag{27}$$

where η remains constant during the closing. To be consistent with the damage model, the residual stresses are zero when $[\![\underline{u}]\!] = \underline{0}$, which leads to

$$\underline{\sigma}_0^s = \underline{0}. \tag{28}$$

Then, the calculation of the stress from the potential yields

$$\underline{\sigma}^s = \frac{\partial \psi_s}{\partial [\![\underline{u}]\!]} = \eta [\![\underline{u}]\!]. \tag{29}$$

One can observe that the chosen expression of the potential (27) enforces the alignment of $\underline{\sigma}^s$ and $[\![\underline{u}]\!]$. Now let us apply the energy balance (22) from the first section to a closing sequence until the displacement jump $[\![\underline{u}]\!]$ becomes zero. This is a nondissipative transformation and the kinetic energy is assumed to be zero; thus, the total energy is

$$\mathscr{E} = \Psi_s - W_{ext}. \tag{30}$$

Therefore, the energy balance of the closing verifies

$$\Delta\Psi_s = \Delta W_{ext}. \tag{31}$$

Let $(1-\lambda)[\![\underline{u}]\!]$ denote the displacement jump of the crack. Initially, $\lambda = 0$; then it increases during closing until $\lambda = 1$. Thus, the local expression of energy conservation can be written as

$$\Delta\psi_s = \int_{\lambda=0}^{1} \underline{\sigma}^s d((1-\lambda)[\![\underline{u}]\!]). \tag{32}$$

Taking (29) into account, we get

$$\Delta\psi_s = -\eta[\![\underline{u}]\!]^2 \int_{\lambda=0}^{1} (1-\lambda)d\lambda, \tag{33}$$

$$\Delta\psi_s = -\frac{1}{2}\underline{\sigma}^s[\![\underline{u}]\!]. \tag{34}$$

Once the material has been completely unloaded ($\lambda = 1$), ψ_s is zero everywhere along the discontinuity. Therefore, the free surface energy before closing verifies

$$\psi_s = \frac{1}{2}\underline{\sigma}^s[\![\underline{u}]\!]. \tag{35}$$

Introducing the free energy calculated in (35) into the expression of the dissipated energy given by Eq. (13), we get

$$d\phi_s = \frac{1}{2}(\underline{\sigma}^s d[\![\underline{u}]\!] - [\![\underline{u}]\!] d\underline{\sigma}^s). \tag{36}$$

We have set up a thermodynamic framework for the cohesive model similar to that which is used for a damage model. Now, the objective for the rest of this paper is to establish a coupling between a continuous damage model and a fracture model. In order to do that, the first step consists in investigating whether such models are capable of representing the same phenomena.

4. Domains of validity of the models being considered

Continuous models provide a very effective means of modeling damage in a material as long as the scalar $d\underline{\underline{\sigma}} : d\underline{\underline{\varepsilon}}$ remains strictly positive. One can show that the loss of positiveness of this quantity coincides with the loss of the material stability and the possible propagation of a zero-velocity wave in the structure (Hadamard, 1903; Hill, 1962). In terms of finite element calculations, one can observe that localization results in the damaged zone being reduced to the size of an element, which makes the problem pathologically dependent on the mesh. In other words, the loss of local stability marks the end of the domain of validity of conventional continuous models.

From an experimental point of view, one can consider that the loss of material stability corresponds to the transition from diffuse damage within the structure to localized damage in the vicinity of the most highly loaded zone of the material. Since diffuse damage, contrary to localized damage, cannot be modeled by a discontinuity, the loss of material stability also marks the beginning of the domain of validity of discontinuous fracture models. One of the main advantages of cohesive models compared to Griffith's fracture models, is that they can detect the initiation of a crack more easily.

It was proved in Charlotte et al. (2000) for the one-dimensional case and in Charlotte et al. (2006) for the three-dimensional case that cohesive models are capable of dealing with the initiation of a discontinuity in an initially healthy structure. In the 3D case, if the potentials are sufficiently regular, the initiation criterion of a discontinuity can be expressed in terms of the principal stresses σ_1, σ_2 and σ_3 as follows:

$$\max_i(\sigma_i) > \sigma_c \ \text{ or } \ \max_{ij}(\sigma_i - \sigma_j) > 2\tau_c \quad \forall (i,j) \in \{1,2,3\}^2, \tag{37}$$

where σ_c and τ_c are constants which characterize the material. We can recognize here the standard Rankine and Tresca initiation conditions.

It would be unrealistic to attempt to solve a diffuse damage problem using a fracture model. As a consequence, the cohesive model, which is capable of dealing with the initiation of a crack, can be considered to be valid as soon as the localized damage phase begins. On the contrary, the damage model is effective in modeling diffuse damage, but poorly suited for modeling localized damage. Finally, the domains of validity of the two models being considered is represented in Fig. 1.

Since coupling must be achieved on the common parts of the domains of validity of the models, coupling a continuous damage model with a fracture model appears difficult. The solution comes from the concept of localization limiter, which enables one, among other things, to extend the domain of validity of the classical damage model to the localized stage of rupture.

The incapability of continuous models to model localized damage is often explained by the fact that they fail to take into account a characteristic length of the material's microstructure. The notion of localization limiter was proposed as a means to solve this problem (Lasry and Belytschko, 1988). The idea was to introduce into the model a characteristic length representing the size of the damaged zone. The numerous ways which have been proposed to introduce such a characteristic length can be classified into two categories.

The first category pertains to discontinuous localization limiters. The idea is to introduce a Griffith-type or cohesive-type crack into the material (Ortiz et al., 1987). One can verify that such a crack plays the role of a localization limiter by observing that the quantity G_c/E, with G_c being the critical elastic energy recovery rate and E the material's Young's modulus, has indeed the dimension of a length.

The second option to limit localization consists in maintaining a continuous description of the material once localization has started, but imposing a minimum size on the damaged zone. In order to do that, some models transgress the damage models' underlying local state assumption and make one or several parameters of the model depend not only on the state of the point under consideration, but also on the state of the neighboring points. Nonlocal models (Pijaudier-Cabot and Bažant, 1987) and second-gradient models (Aifantis, 1984), which can be viewed as a subset of nonlocal models (Bažant et al., 1984; Peerlings et al., 2001), belong in this category. It is also possible to introduce some degree of viscosity into the material's behavior, as in delay-effect models (Ladevéze, 1992). In the rest of this work, we will focus more specifically on nonlocal models, which we are now going to present in more detail.

In order to use a nonlocal model, the first step consists in choosing one or several internal variables to be regularized. Let z be one of these internal variables. The regularized variable $\bar{z}$ is defined by

$$\bar{z}(\underline{x}) = \frac{1}{V(\underline{x})} \int_\Omega z(\underline{s})\alpha(\underline{s}-\underline{x})dV \tag{38}$$

with

$$V(\underline{x}) = \int_\Omega \alpha(\underline{s}-\underline{x})dV. \tag{39}$$

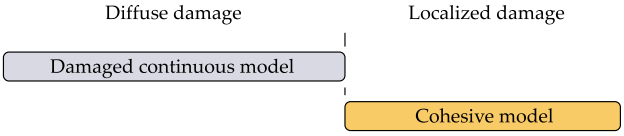

Fig. 1. Domains of validity of the continuous and discontinuous models.

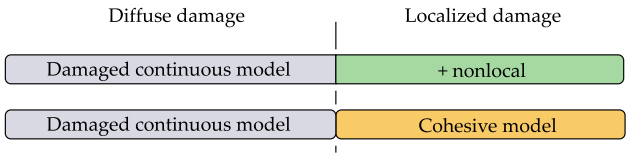

Fig. 2. Domains of validity of the continuous and discontinuous models.

α is a weight function, such as a Gauss function

$$\alpha(\underline{s}-\underline{x}) = \exp\left(-\left(\frac{k\|\underline{s}-\underline{x}\|}{l_c}\right)^2\right). \tag{40}$$

l_c being the characteristic length of the material's microstructure.

When dealing with the general case of rupture involving a diffuse damage phase and a localized damage phase, it seems attractive to have at one's disposal models which are effective enough to simulate the whole rupture process. For the diffuse damage phase, this is possible only if one uses a continuous model. For the localized phase, one can choose between a discontinuous model of the cohesive zone type (the only one capable of detecting the initiation of the crack) or a continuous model equipped with a means of limiting localization. In the following sections, we will attempt to couple a nonlocal damage model with a classical damage model in which we allow the formation of a discontinuity of the cohesive zone type. The domains of validity of these two models can be represented in Fig. 2.

The next step consists in establishing the coupling between the two methods chosen to limit localization in the material.

5. The model coupling method

5.1. Existing methods and objectives

5.1.1. The "mechanical" approach to coupling

This approach, developed by Planas et al. (1993), is based on the strong discontinuity method (Simo et al., 1993), which uses Heaviside-type functions to introduce discontinuities into the displacement field of the structure. The strain field is obtained by derivation of this discontinuous field in the distribution sense. Thus, at the discontinuity, one gets the strain in the form of a finite second-order tensor multiplied by a Dirac function. This strain field can be viewed as a localized field, which can be smoothed as in the case of a nonlocal model. The coupling method is based on the fact that even though the initial strain field is discontinuous the regularized strain field thus obtained is continuous: the smoothing stage provides the transition from a discontinuous field to a continuous field. Thus, one obtains an effective method of coupling continuous and discontinuous models.

In order to apply this method, a first approach would be to start from a continuous nonlocal model and seek discontinuous local fields which reproduce the regularized strain field of the nonlocal model. This application was developed in Planas et al. (1993) to seek analytical solutions of cohesive models which would be equivalent to solutions of nonlocal models. Legrain et al. (2007) used the method with a purely numerical approach, following a nonlocal damage calculation, in order to extract the crack's displacement jump. The method can also be used to build one-dimensional analytical solutions of nonlocal models, as did Legrain et al. (2007) to get a reference solution of the nonlocal damage problem.

For one-dimensional problems, the use of this method is relatively straightforward. For three-dimensional problems, the integration of the variable to be regularized must be carried out perpendicular to the crack's surface. We would use this approach to coupling in order to build analytical solutions of nonlocal models from discontinuous fields. For the purpose of coupling models, we prefer to use a method based on an "energy" approach which we are going to present next.

5.1.2. The "energy" approach to coupling

Another approach to the coupling problem consists in trying to obtain two thermodynamically equivalent models. Mazars (1984) proposed to seek the same dissipated energy in a damage model and in a Griffith fracture model. This idea was taken up by Mazars and Pijaudier-Cabot (1996), this time using a nonlocal damage model. Let us give a brief summary of this method which will be the basis of the rest of our work. For Griffith's model, the increment of dissipated energy is

$$d\Phi = G_c\, d\mathscr{A}, \tag{41}$$

where G_c is the critical elastic energy recovery rate and $\mathscr{A}$ the area of the crack. For the damage model, the increment of dissipated energy is

$$d\Phi = \int_\Omega (-Y\, dD) dV, \tag{42}$$

where Y is the elastic energy recovery rate defined by

$$Y = \frac{\partial \psi}{\partial D}. \tag{43}$$

Writing that these two expressions of dissipation are equal, we get the following relation:

$$d\mathscr{A} = \frac{\int_\Omega (-Y\, dD) dV}{G_c}. \tag{44}$$

Then, this expression can be integrated over time in order, for example, to verify that the parameters of a damage model agree with a given critical elastic energy recovery rate for the same material. As suggested by Mazars (1984), one can also use a cohesive model instead of a Griffith model based on the fact, according to Rice (1968) and Hillerborg et al. (1976), that the area under the traction curve of the cohesive model is equal to G_c:

$$G_c = \int_0^\infty \underline{\sigma}^s d[\![\underline{u}]\!]. \tag{45}$$

Comi et al. (2002, 2007) used this method along with a numerical resolution based on enriched finite elements. We can also point out that Bažant and Oh (1983) relate the crack band model to the cohesive fracture model by enforcing an equality between the consumed energy of both model.

5.2. Energy criterion for model coupling

The objective of the rest of this study is to apply the "energy" coupling method with a cohesive model which is well-defined thermodynamically and for which no assumption is made on the shape of the cohesive law. The energy criterion we chose for this coupling is a global criterion over the whole structure which can be expressed as

$$\hat{\Phi} = \breve{\Phi}. \tag{46}$$

$\breve{\Phi}$ being the energy dissipated by the structure for a nonlocal damage model and $\hat{\Phi}$ the energy dissipated in the case of a classical damage model in which one allows the formation of a cohesive zone. In $\hat{\Phi}$, let us make a distinction between the energy dissipated in the volume $\hat{\Phi}_{vol}$ and the energy dissipated at the discontinuity $\hat{\Phi}_s$:

$$\breve{\Phi} = \hat{\Phi}_{vol} + \hat{\Phi}_s. \tag{47}$$

Thus, the energy dissipated by the cohesive zone is equal to

$$\hat{\Phi}_s = \breve{\Phi} - \hat{\Phi}_{vol}. \tag{48}$$

Now let us consider two cases. Looking at the situation prior to localization, the only existing damage in the material is diffuse damage, on which the nonlocal model has little or no effect. Then, one can assume that $d\breve{\Phi} = d\hat{\Phi}_{vol}$, i.e.

$$d\hat{\Phi}_s = 0 \quad \text{before localization.} \tag{49}$$

However, after localization, the opening of the cohesive zone tends to unload the material in the vicinity of the cracked zone. Then, one can assume that $d\hat{\Phi}_{vol} = 0$, i.e.

$$d\hat{\Phi}_s = d\breve{\Phi} \quad \text{after localization.} \tag{50}$$

Those increments of dissipated energy are the only pieces of information that will be used to construct the discrete model of fracture from the knowledge of the continuous damage model.

5.3. Choice of the cohesive model to be used

Since the global unloading behavior of the nonlocal damage model is linear, it is natural to enforce the same behavior for the model which combines "classical" damage and a cohesive zone. Therefore, we will use the cohesive model with linear closing introduced before. Thus, we can use expression (36) for the increment of dissipated energy. In the one-dimensional case, or if the cohesive zone is loaded in Mode I alone, one can define σ^s and $[\![u]\!]$ such that

$$\underline{\sigma}^s = \sigma^s \underline{n}, \tag{51}$$

$$[\![\underline{u}]\!] = [\![u]\!]\underline{n}. \tag{52}$$

Then, the increment of dissipated surface energy becomes

$$d\hat{\phi}_s = \frac{1}{2}(\sigma^s d[\![u]\!] - [\![u]\!] d\sigma^s) \tag{53}$$

and can be represented by diagram 3.

5.4. Verification of the energy equivalence of the two models

Let us go back to the global energy balance (22) for a problem in which the inertia terms are negligible:

$$\mathscr{E} = \Psi - W_{ext} + \Phi. \tag{54}$$

We set out to couple the two models based on the conservation of the dissipated energy. Let $\breve{(\cdot)}$ denote the quantities associated with the nonlocal damage model, and $\hat{(\cdot)}$ the quantities associated with the "classical" damage model which can be run across by a cohesive zone. In order to show that the two models are equivalent energy-wise, we must show that each term of the energy balance is the same with the two models, i.e.

$$(\hat{\mathscr{E}}, \hat{\Psi}, \hat{W}_{ext}, \hat{\Phi}) = (\breve{\mathscr{E}}, \breve{\Psi}, \breve{W}_{ext}, \breve{\Phi}) \quad \forall t. \tag{55}$$

In order to achieve this energy equivalence, we propose to enforce equal energy dissipation for the two models, i.e.

$$\hat{\Phi} = \breve{\Phi} \quad \forall t. \tag{56}$$

In addition, since the total energy $\mathscr{E}$, by definition, does not vary over time and is defined to within an arbitrary constant, one can consider that

$$\hat{\mathscr{E}} = \breve{\mathscr{E}} \quad \forall t. \tag{57}$$

Thus, only the conservation of Ψ and W_{ext} between the two models remains to be shown. Since the energy balance (54) is verified in both cases, it suffices to verify the property for one of the two quantities for the other to be verified automatically. Let us prove the energy equivalence by induction using a problem discretized in time. Energy equivalence between the two models is assumed at time t, i.e.

$$(\hat{\Psi}^t, \hat{W}^t_{ext}) = (\breve{\Psi}^t, \breve{W}^t_{ext}). \tag{58}$$

We want to show that this equality remains true at time $t + dt$. The problems associated with the two models have the same boundary conditions. The unloading behavior of the nonlocal damage model is linear. This property also holds for the model which associates damage and a cohesive zone because a cohesive model with linear closing was chosen. Thus, the stored elastic energy inside the structure bounded by Γ can be calculated using the following integral:

$$\Psi^t = \frac{1}{2}\int_\Gamma \underline{F}^t \underline{u}^t \, dS. \tag{59}$$

From expression (54) of the total energy, we know that

$$d\Phi = dW_{ext} - d\Psi. \tag{60}$$

Therefore, the increment of energy dissipated by the structure is

$$d\Phi = \frac{1}{2}\int_\Gamma (\underline{F}^t \, d\underline{u} - \underline{u}^t \, d\underline{F}) dS. \tag{61}$$

Let us assume that the boundary conditions consist only of prescribed displacements at the boundary of the structure ($\Gamma_1 = \Gamma$ et $\Gamma_2 = \varnothing$) and can be defined through a unit reference loading represented by the field $\underline{u}_0$ and a loading coefficient λ.

$$\hat{\underline{u}} = \breve{\underline{u}} = \underline{u} = \lambda \underline{u}_0 \quad \text{over } \Gamma. \tag{62}$$

Therefore, the loading increment is

$$d\hat{\underline{u}} = d\breve{\underline{u}} = d\underline{u} = d\lambda \underline{u}_0 \quad \text{over } \Gamma. \tag{63}$$

Since the increment of dissipated energy is the same for the two models, one can write

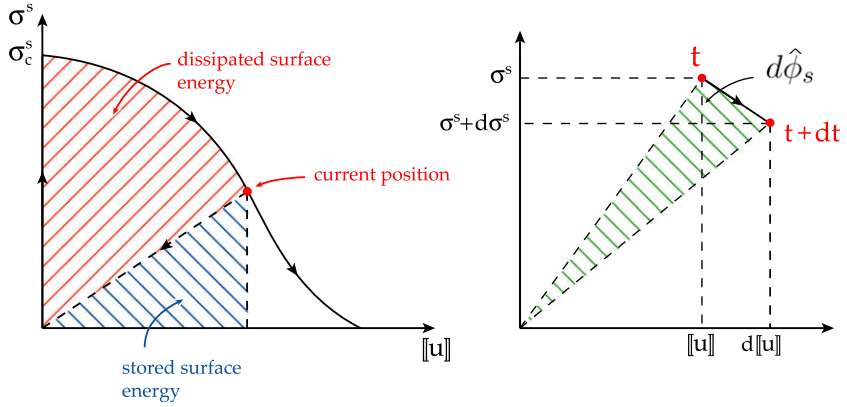

Fig. 3. Increment of dissipated energy in the cohesive zone.

$$\int_\Gamma (\hat{\underline{F}}^t\, d\lambda - \lambda^t\, d\hat{\underline{F}})\underline{u}_0\, dS = \int_\Gamma (\breve{\underline{F}}^t\, d\lambda - \lambda^t\, d\breve{\underline{F}})\underline{u}_0\, dS. \tag{64}$$

Besides, from (58), we know that at time t, $\hat{\Psi}^t = \breve{\Psi}^t$; therefore, from (59)

$$\int_\Gamma \hat{\underline{F}}^t \underline{u}^t\, dS = \int_\Gamma \breve{\underline{F}}^t \underline{u}^t\, dS. \tag{65}$$

Thus, we get

$$\int_\Gamma \hat{\underline{F}}^t \underline{u}_0\, dS = \int_\Gamma \breve{\underline{F}}^t \underline{u}_0\, dS. \tag{66}$$

This equation allows relation (64) to be simplified to

$$\int_\Gamma d\hat{\underline{F}}\underline{u}_0\, dS = \int_\Gamma d\breve{\underline{F}}\underline{u}_0\, dS. \tag{67}$$

Therefore

$$\int_\Gamma \hat{\underline{F}}^{t+dt}\underline{u}_0\, dS = \int_\Gamma \breve{\underline{F}}^{t+dt}\underline{u}_0\, dS, \tag{68}$$

which shows that relation (65) remains valid at time $t + dt$:

$$\int_\Gamma \hat{\underline{F}}^{t+dt}\underline{u}^{t+dt}\, dS = \int_\Gamma \breve{\underline{F}}^{t+dt}\underline{u}^{t+dt}\, dS \tag{69}$$

and, therefore, that $\hat{\Psi}^{t+dt} = \breve{\Psi}^{t+dt}$. Thus, the free energy at time $t + dt$ is the same for both models. Using the energy balance (54), we also get that the work of the external loads is the same for both models. The induction relation holds true at time $t + dt$:

$$(\hat{\Psi}^{t+dt}, \hat{W}_{ext}^{t+dt}) = (\breve{\Psi}^{t+dt}, \breve{W}_{ext}^{t+dt}). \tag{70}$$

We assume that the two models are identical with regard to the elastic part of the material's behavior, which enables us to initiate induction. A proof similar to what we have just done shows the energy equivalence in the case of a loading in terms of prescribed forces based on a reference loading case.

5.5. Case of a softening behavior

If the material degradation occurs with localized damage alone, the study of model coupling is simplified. This is an interesting case because it enables one to deal only with the rupture stage during which model coupling is being achieved. The continuous model which corresponds to localized damage alone is a damage model whose traction curve presents a peak following the elastic phase. For example, if one looks at Mazars' damage model Mazars, 1984, whose behavior is different in traction and in compression: cf. Fig. 4. One can see that rupture under traction loading can be considered to be localized. Therefore, the only equation to be used for coupling is Eq. (50). In this case, the material remains free from damage in the vicinity of the cohesive zone ($\hat{\Phi}_{vol} = 0$).

6. Application to the automatic determination of a cohesive law by an incremental method

6.1. Objective

The objective of this section is, for one-dimensional examples, to calculate a cohesive law given a nonlocal damage model. We assume that the location of the discontinuity is known *a priori*. The cohesive model is built automatically, in incremental fashion, from the surface energy dissipation obtained through Eqs. (49) and (50). The incremental construction of the cohesive model is represented in Fig. 5.

The nonlocal calculation starts by assuming that the strain in the beam is homogeneous, then by considering an analytical solution of the nonlocal model. The homogeneous strain assumption in the beam during the localization phase is acceptable only if the size of the beam is smaller than the width of the localization zone. This is not a very satisfactory assumption, but it is the only hypothesis leading to a relatively simple calculation of the differential equations describing the evolution of the macroscopic structure's behavior over time. The solution is obtained either through analytical differential equations, or through a numerical resolution method using a Lagrange multiplier to describe the boundary conditions being applied at the level of the discontinuity. The latter method enables one to solve the two models independently of each other and can be used in a FEM framework.

Three examples, whose particularities are summarized in Table 1, will be presented in this paper. The aim of the first example (6.2) is to present the direct calculation of the cohesive zone traction law from analytical differential equations. In the second and third examples (6.4 and 6.5), the equivalent discontinuous model is obtained numerically with the method presented in Section 6.3. The particularity of the second example is that it has a stable propaga-

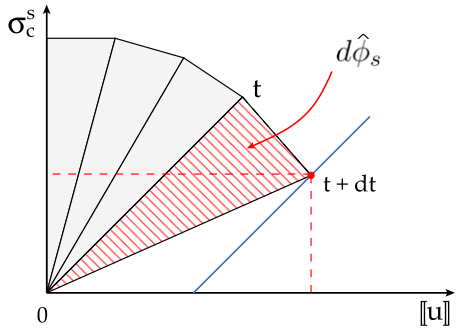

Fig. 5. Incremental calculation of the cohesive model.

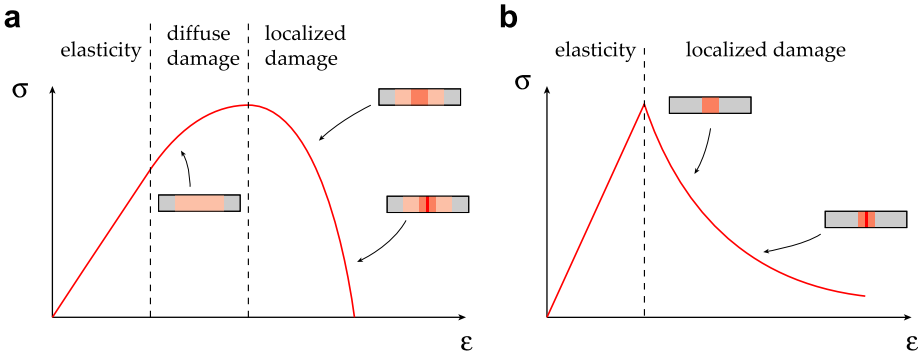

Fig. 4. $\sigma = f(\varepsilon)$ curve under compression loading (a) and traction loading (b).

Table 1
Details of the developed examples.

	Reference model		Equivalent model
	Regularization method	Stability of damage	Resolution method
Example 1 (6.2)	Homogeneous	Unstable	Differential equations
Example 2 (6.4)	Homogeneous	Stable and unstable	Numerical (6.3)
Example 3 (6.5)	Nonlocal (analytical)	Unstable	Numerical (6.3)

tion phase before localization so that Eqs. (49) and (50) are both used during the resolution.

6.2. Case of a simple localized damage problem: strong formulation

The objective is to solve the one-dimensional problem of a beam of length L, cross-section S and Young's modulus E subjected to a traction loading over a time period between 0 and t_{max}. The behavior of the material is represented through a damage model in which the damage variable is assumed to be homogeneous within the beam, which is a crude way of preventing localization. Besides, a second model considers that the beam consists of an elastic material which can be cut by a discontinuity in its center (localized fracture case). The beam is clamped on the left and subjected to a prescribed displacement u_r at the point of abscissa $x = L$ (cf. Fig. 6).

The prescribed displacement u_r verifies a linear loading law governed by a parameter, denoted a, such that

$$u_r = at. \tag{71}$$

The damageable model depends on the maximum strain κ in the beam over time

$$\kappa = \max_t(\varepsilon) \tag{72}$$

and verifies a piecewise linear behavior as in Fig. 7.

Thus, the damage variable verifies

$$D = 0 \quad \text{if } \kappa < \varepsilon_0, \tag{73}$$

$$D = \frac{\kappa - \varepsilon_0}{\varepsilon_r - \varepsilon_0} \quad \text{if } \varepsilon_0 \leqslant \kappa \leqslant \varepsilon_r, \tag{74}$$

$$D = 1 \quad \text{if } \kappa > \varepsilon_r. \tag{75}$$

Parameter a is chosen such that at the end of the simulation the material is fully damaged ($D = 1$). In order to enforce localized damage, we want the model to enter an unstable damage phase as soon as it leaves the elastic domain. In order to do that, we use the material stability criterion:

$$d\sigma\, d\varepsilon > 0. \tag{76}$$

If one chooses $\varepsilon_0 = \varepsilon_r/2$, the localization occurs from the beginning of the damaged state. We used the following parameters for the problem: $L = 1$ m, $S = 10^{-2}$ m^2, $E = 40$ GPa, $\varepsilon_0 = 10^{-4}$, $\varepsilon_r = 2\times 10^{-4}$, $t_{max} = 3$ s. Fig. 8 shows the corresponding traction curve.

The stress of the damage model, denoted $\breve{\sigma}$ and assumed to be homogeneous within the material, is given by

$$\breve{\sigma} = (1 - D)E\varepsilon. \tag{77}$$

Since the strain in the beam increases, $\kappa = \varepsilon$ and the stress can be written as

$$\breve{\sigma} = E\varepsilon \quad \text{if } \varepsilon \leqslant \varepsilon_0, \tag{78}$$

$$\breve{\sigma} = \frac{\varepsilon_r - \varepsilon}{\varepsilon_r - \varepsilon_0} E\varepsilon \quad \text{if } \varepsilon > \varepsilon_0. \tag{79}$$

The variation of dissipated energy $d\breve{\Phi}$ is equal to

$$d\breve{\Phi} = \int_\Omega (-Y\, dD) dV, \tag{80}$$

where Y is the elastic energy recovery rate, which for a beam in traction, is equal to

$$Y = -\frac{1}{2} E\varepsilon^2. \tag{81}$$

Denoting t_0 the time of transition between the diffuse phase and the localized phase (here, $t_0 = t_{max}/2$), one gets

$$d\breve{\Phi} = 0 \quad \text{if } t \leqslant t_0, \tag{82}$$

$$d\breve{\Phi} = \frac{1}{2} ES\, \frac{u_r^2}{L^2} \frac{du_r}{\varepsilon_r - \varepsilon_0} \quad \text{if } t > t_0. \tag{83}$$

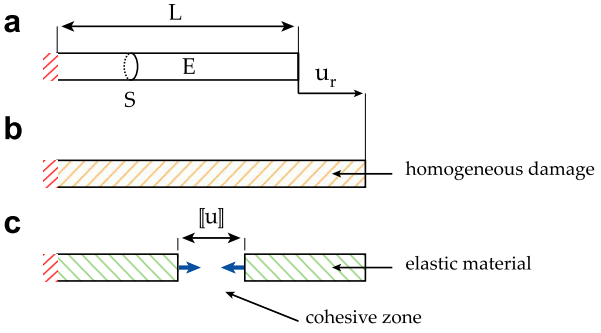

Fig. 6. (a) The problem to be solved, (b) homogeneous damage model and (c) cohesive model.

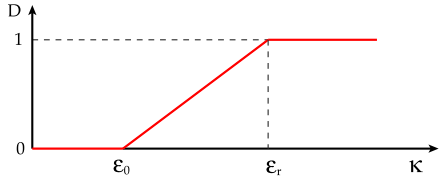

Fig. 7. Evolution of the damage variable.

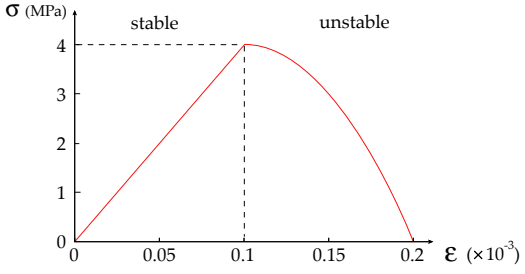

Fig. 8. Traction curve of the damage model.

Let us now consider the cohesive model for which the increment of dissipated energy is given by Eq. (53). If $\hat{\sigma}$ denotes the stress in the material in the vicinity of the cohesive zone, the equilibrium of the structure in that zone requires that $\sigma^s = \hat{\sigma}$. Since we are dealing with a localized fracture problem, the material near the cohesive zone behaves elastically, which leads to the following expression of $\hat{\sigma}$ and σ^s:

$$\sigma^s = \hat{\sigma} = \frac{u_r - [\![u]\!]}{L} E. \tag{84}$$

Finally, we want to have identical energy dissipation between the two models. Since we are in a localized damage case, we may simply use relation (50), which, in this case, can be written as

$$d\hat{\phi}_s = \frac{d\breve{\Phi}}{S}. \tag{85}$$

These equations introduced in Eq. (53) lead to the following differential equations:

$$d[\![u]\!] = 0 \quad \text{if } t \leqslant t_0, \tag{86}$$

$$d[\![u]\!] = \frac{1}{t}\left(\frac{a^2 t^2}{L(\varepsilon_r - \varepsilon_0)} + [\![u]\!]\right) dt \quad \text{if } t > t_0. \tag{87}$$

In order to verify the validity of the previous equations, we carried out a numerical calculation. We used a Euler-type resolution method to solve Eqs. (86) and (87) explicitly and compared the result to that of the damageable calculation. The calculations presented here were carried out with 100 time steps. The first curve 9(a) shows the evolution over time of the prescribed displacement of the beam's end and of the displacement jump at the discontinuity. The second curve 9(b) shows the evolution of the stress σ^s in the cohesive model as a function of the displacement jump, which corresponds to the behavior law of the cohesive zone. One can verify that this curve is identical to that which represents the stress $\breve{\sigma}$ of the damage model.

The third curve 10(a) shows the dissipated energy for each model as a function of time, which enables one to verify that the compatibility condition between the two models is satisfied. The fourth curve 10(b) shows the free energy in the material as a function of time for the two models. For the cohesive model, this is the sum of the strain energy of the elastic zone and the free energy of the cohesive zone. Again, the two curves are identical, which enables one to check the energy equivalence of the two models (proven in 5.4).

The fact that curves are not perfectly superposed is due to numerical errors. This can easily be improved by increasing the number of time steps.

Remark: In this particular case, the differential equations (86) and (87) have an analytical solution, which gives the following expression for the displacement jump $[\![u]\!]$:

$$[\![u]\!] = 0 \quad \text{if } t \leqslant t_0, \tag{88}$$

$$[\![u]\!] = \frac{a^2 t}{L(\varepsilon_r - \varepsilon_0)}(t - t_0) \qquad \text{if } t > t_0. \tag{89}$$

With the data we used, the numerical solution and the analytical solution agree perfectly.

6.3. General resolution based on an energy method

6.3.1. Derivation of the continuous problem

Now we will try to develop a resolution method for the damage problem with a crack, starting from a weak formulation of the problem. The objective is to obtain a method in which the resolution of each of the two models is carried out separately. The only piece of information which circulates between the nonlocal model and the cohesive zone model is the dissipated energy $\hat{\Phi}_s$ detected by the cohesive zone. Let us isolate the volume part of the structure, so that the cohesive forces can be viewed as external loads

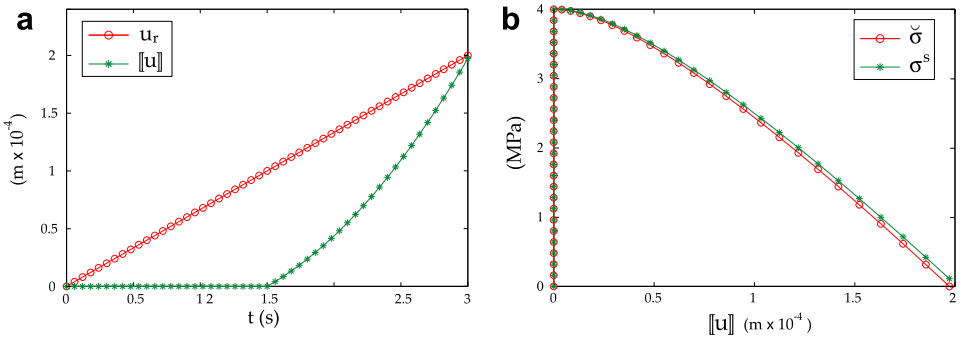

Fig. 9. (a) Displacement of the beam's end and displacement jump for the cohesive model and (b) traction curve of the cohesive model.

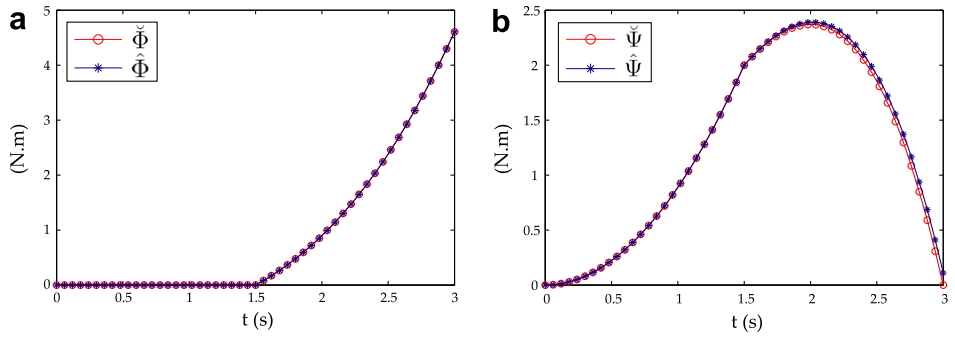

Fig. 10. Verification of the energy equivalence for the dissipated energy (a) and the free energy (b).

applied to the system. We assume that the crack appears at the point of abscissa x_0. The beam is built-in on the left and, therefore, the displacement $u_l = u(0)$ is zero. Let $u_r = u(L)$ denote the prescribed displacement at the beam's right-hand cross-section and F the corresponding load (cf. Fig. 11).

Taking the solution field as the virtual field, the principle of virtual power can be written as follows:

$$S\int_{[0,L]\setminus x_0}(d\sigma\, d\varepsilon)dx = dF\, du_r - S d\sigma^s d[\![u]\!]. \tag{90}$$

The prescribed displacement is handled through a Lagrange multiplier λ such that

$$\lambda = -F \tag{91}$$

and we define the restriction operators A_l and A_r which give, when applied to the field u, the displacement of the right and the left edge of the beam:

$$A_l(u) = u(0) = 0, \tag{92}$$

$$A_r(u) = u(L) = u_r. \tag{93}$$

The increment in the stress field $d\sigma$ can be calculated from the material's tangent modulus C:

$$d\sigma = C\, d\varepsilon. \tag{94}$$

Then, the incremental expression of the principle of virtual power (90) becomes

$$S\int_{[0,L]\setminus x_0} C\, d\varepsilon^2\, dx = -d\lambda A_r(du) - S d\sigma^s d[\![u]\!]. \tag{95}$$

In addition, the solution of the incremental problem must verify the coupling condition for the increment of dissipated energy $d\hat{\Phi}$ which, from 53, can be written as

$$d\hat{\Phi} = \frac{S}{2}(\sigma^s d[\![u]\!] - [\![u]\!] d\sigma^s) \tag{96}$$

and must verify the displacement boundary conditions (Eqs. (92) and (93)). We consider the discontinuity to be a surface with prescribed displacements: therefore, we must add to the problem a multiplier μ associated with the discontinuity representing the cohesion stresses and defined by

$$\mu = S\sigma^s. \tag{97}$$

Thus, the unknowns of the problem are

$$u \quad \text{for } x \in [0, L] \setminus x_0, \tag{98}$$

$$\lambda \quad \text{for } x = L, \tag{99}$$

$$\mu \quad \text{for } x = x_0. \tag{100}$$

Operator T is defined such that

$$T(u) = [\![u]\!]. \tag{101}$$

Then, expression (95) of the principle of virtual power can be written as

$$S\int_{[0,L]\setminus x_0} C\, d\varepsilon^2\, dx + d\lambda A_r(du) + d\mu T(du) = 0. \tag{102}$$

The additional equations which need to be verified are, on the one hand, Eqs. (92) and (93) representing the displacement boundary conditions and, on the other hand, Eq. (96), which is used to determine the increment in displacement jump $d[\![u]\!]$ which, because of (97), can be written as

$$d[\![u]\!] = \frac{[\![u]\!]d\mu + 2d\hat{\Phi}}{\mu}. \tag{103}$$

We use the following definitions of m and v (which are known at time t):

$$m = \frac{[\![u]\!]}{\mu} \quad \text{and} \quad dv = \frac{d\hat{\Phi}}{\mu}, \tag{104}$$

which enables us to rewrite (103) in the form

$$d[\![u]\!] = m d\mu + 2dv. \tag{105}$$

6.3.2. Discretization of the problem

Let us apply the energy method to the localized damage problem considered previously (6.2). The discretization we used has four degrees of freedom numbered 1–4, and can be represented as follows: cf. Fig. 12.

Eqs. (102), (93) and (105), after spatial discretization, lead to a system of the form

$$\begin{pmatrix} K & A^T & T^T \\ A & 0 & 0 \\ T & 0 & -M \end{pmatrix}\begin{pmatrix} dU \\ d\lambda \\ d\mu \end{pmatrix} = \begin{pmatrix} 0 \\ dU_d \\ 2dV \end{pmatrix}. \tag{106}$$

Then, this problem must be discretized over time in order to be solved numerically. Since the volume problem can be nonlinear in the case of not only localized damage, a Newton algorithm is used to go from one time step to the next. This method of resolution leads to the same results as the integration of the analytical differential equations obtained in 6.2. The following plot superimposes the displacement jumps obtained with the two methods as functions of time (cf. Fig. 13).

6.4. Case of a damage model with a diffuse damage phase

Let us now reconsider the previous test (6.2) and modify the parameters of the damage model in order to create a diffuse damage phase prior to the localized damage phase. All we need to do is increase ε_r while keeping the other parameters of the model the same. Thus, we choose a slightly higher rupture strain ($\varepsilon_r = 3 \times 10^{-4}$) and keep the other parameters of the problem unchanged. Fig. 14 shows the traction curve corresponding to this choice of the material's parameters.

One can verify the presence of a hardening damage zone corresponding to the diffuse damage and a softening zone corresponding to the localized damage. This delay between the beginning of damage and the localization must be taken into account in building

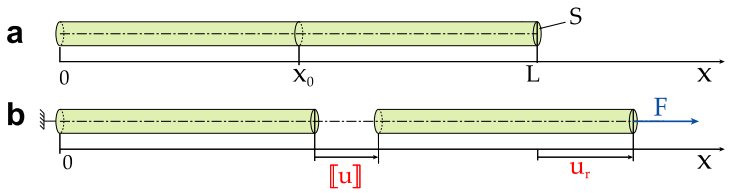

Fig. 11. The beam's geometry before (a) and after deformation (b).

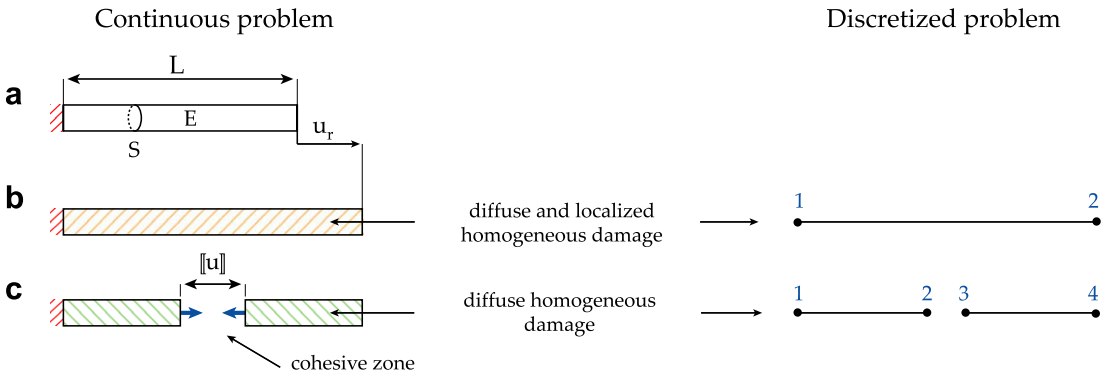

Fig. 12. Separate resolution of the models.

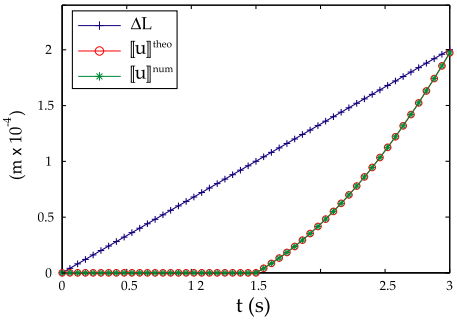

Fig. 13. Superposition of the displacement jumps obtained with the two methods.

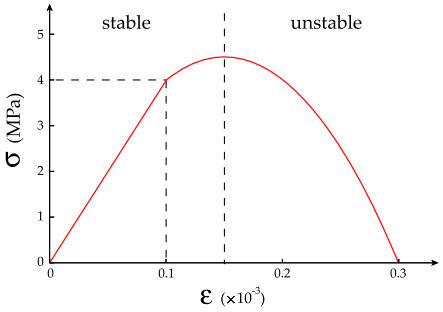

Fig. 14. Traction curve of the damage model.

the cohesive model. Coupling of the models is achieved through Eq. (49) during the diffuse damage phase, then Eq. (50) during the localized damage phase. We still assume that damage is homogeneous within the beam. For the resolution, we use the energy method proposed in 6.3. We can again plot the displacement jump at the crack as a function of time in Fig. 15(a) and the behavior law of the cohesive model in Fig. 15(b).

Curve 16(a) also enables us to verify that the coupling criterion based on the localized dissipated energy is satisfied. On the same curve, we also plotted the total dissipated energy for the two models, which enables us to verify that, for that energy, the energy balance is satisfied. Curve 16(b) shows that the energy correspondence also holds for the free energy.

6.5. Use of a true nonlocal damage model

6.5.1. Definition of the nonlocal damage problem

In this section, we calculate a cohesive law using a true nonlocal damage model based on a strain field smoothed by a Gauss function. Using the "mechanical" approach to model coupling (5.1.1), we obtain an analytical solution of the nonlocal model. Thus, we assume that the analytical solution of the nonlocal strain field $\bar{\varepsilon}(x)$ can be deduced from a reference displacement field $u(x)$ which is discontinuous at a point of abscissa x_0. This method prevents us to do a numerical calculation of the nonlocal problem on a fine mesh. As before, the beam is built-in at $x = 0$ and subjected to a prescribed displacement u_r at $x = L$, the resulting force at the same point being designated by F. Since the field $u(x)$ must be statically admissible, we have

$$E\frac{du}{dx} = \frac{F}{S} \quad \text{for } x = 0 \text{ and } x = L, \tag{107}$$

$$\frac{d^2u}{dx^2} = 0 \quad \text{forall } x \in [0, L] \setminus x_0. \tag{108}$$

Therefore, the associated strain field is homogeneous over $[0, L] \setminus x_0$. Denoting this strain ε^{hom}, the following expression of $u(x)$ is obtained:

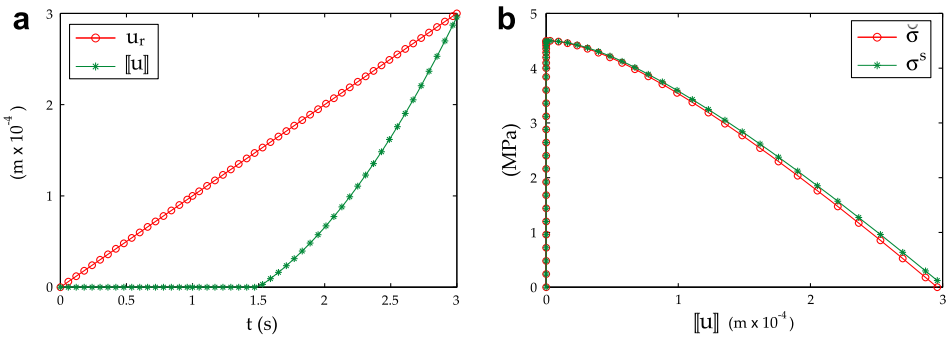

Fig. 15. (a) End displacement of the beam and displacement jump of the cohesive model and (b) traction curve of the cohesive model.

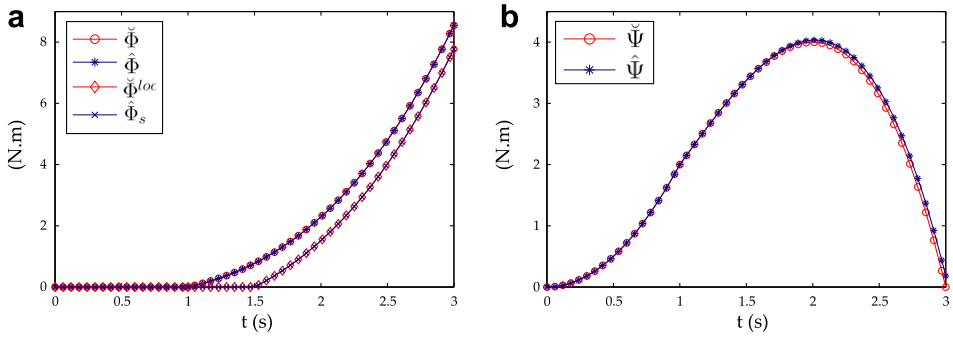

Fig. 16. Verification of the energy equivalence for the dissipated energy (a) and the free energy (b).

$$u(x) = \varepsilon^{hom} x + [\![\breve{u}]\!] H(x - x_0), \tag{109}$$

where H is the Heaviside function. By deriving this displacement field with respect to x in the distribution sense, we obtain the following strain field over $[0, L]$:

$$\varepsilon(x) = \varepsilon^{hom} + [\![\breve{u}]\!] \delta(x - x_0). \tag{110}$$

δ being the Dirac function. It is this strain field that we use to calculate the regularized strain field $\bar{\varepsilon}$:

$$\bar{\varepsilon}(x) = \frac{1}{V(x)} \int_0^L \alpha(s - x)\varepsilon(s) ds \tag{111}$$

with

$$V(x) = \int_0^L \alpha(s - x) ds, \tag{112}$$

where α is the following Gauss function:

$$\alpha(s - x) = \exp\left(\frac{-4(s - x)^2}{l_c^2}\right) \tag{113}$$

l_c is the characteristic length, which depends on the material. Taking into account expression (110) of the strain, one obtains

$$\bar{\varepsilon}(x) = \varepsilon^{hom} + \frac{[\![\breve{u}]\!]}{V(x_0)} \alpha(x - x_0). \tag{114}$$

Let us note that at x_0 the regularized strain is

$$\bar{\varepsilon}(x_0) = \varepsilon^{hom} + \frac{[\![\breve{u}]\!]}{V(x_0)}. \tag{115}$$

We assume that the material follows the behavior of Mazars' damage model Mazars, 1984. With this model, damage depends on an equivalent strain ε_{eq} which, in the one-dimensional case, is defined as follows (Fig. 17):

$$\varepsilon_{eq} = 0 \quad \text{if } \varepsilon \leqslant 0, \tag{116}$$

$$\varepsilon_{eq} = \varepsilon \quad \text{if } \varepsilon > 0. \tag{117}$$

Then, we define a memory variable κ which holds the maximum value over time of the equivalent strain:

$$\kappa = \max_t(\varepsilon_{eq}). \tag{118}$$

In the case of a traction loading, the calculation of the damage variable is carried out as follows:

$$D = 0 \quad \text{if } \kappa \leqslant \varepsilon_0, \tag{119}$$

$$D = 1 - \frac{\varepsilon_0(1 - A_t)}{\kappa} - \frac{A_t}{\exp(B_t(\kappa - \varepsilon_0))} \quad \text{if } \kappa > \varepsilon_0, \tag{120}$$

where ε_0, A_t and B_t are parameters of the material. The stress $\breve{\sigma}$ is given by

$$\breve{\sigma} = (1 - D)E\bar{\varepsilon}. \tag{121}$$

In our calculations, we used the following geometrical parameters: $L = 1$ m, $S = 10^{-2}$ m^2, $x_0 = 0.5$ m, and the following material parameters: $E = 40$ GPa, $\varepsilon_0 = 10^{-4}$, $A_t = 1$, $B_t = 15,000$ and $l_c = 0.3$ m.

6.5.2. Resolution of the nonlocal damage problem

The most natural way to solve the nonlocal damage problem would be to assign, as we did before, a linear prescribed displacement loading law as a function of time. This method works well if the displacement u_r keeps increasing over time, but poses problems in case of snap-back, which requires that the displacement jump be reduced at certain points of the time evolution. We adopted a solution which consists in controlling the calculation through the maximum strain $\bar{\varepsilon}(x_0)$ in the beam. Thus, the loading parameter b is chosen such that

$$\bar{\varepsilon}(x_0) = bt. \tag{122}$$

Since $\bar{\varepsilon}(x_0)$ is positive and increases over time, Eqs. (116)–(118) lead to

$$\kappa(x_0) = \bar{\varepsilon}(x_0). \tag{123}$$

Therefore, from (120) and (121), the stress at x_0 is obtained using the relations

$$\breve{\sigma}(x_0) = E\bar{\varepsilon}(x_0) \quad \text{if } \bar{\varepsilon}(x_0) \leqslant \varepsilon_0, \tag{124}$$

$$\breve{\sigma}(x_0) = E\left(\varepsilon_0(1 - A_t) + \frac{A_t\bar{\varepsilon}(x_0)}{\exp(B_t(\bar{\varepsilon}(x_0) - \varepsilon_0))}\right) \quad \text{if } \bar{\varepsilon}(x_0) > \varepsilon_0. \tag{125}$$

This stress is constant over the whole length of the beam (static admissibility). As one moves away from point $x = x_0$, the strain

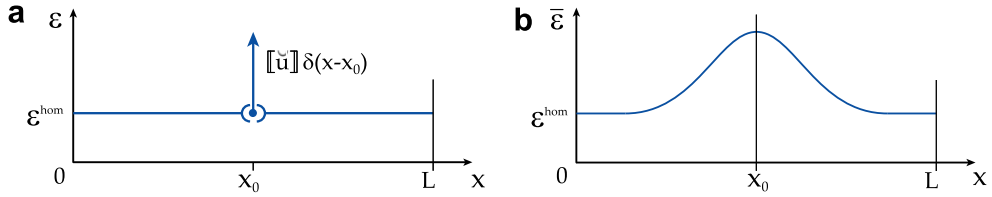

Fig. 17. The strain field before (a) and after smoothing (b).

tends toward ε^{hom}. Since Mazars' model corresponds, in traction, to localized damage only ($\breve{\sigma}$ reaching a maximum at ε_0), we know that far away from x_0 the material is not damaged. Thus, one has $\breve{\sigma} = E\varepsilon^{hom}$, which leads to the following expression for ε^{hom}:

$$\varepsilon^{hom} = \frac{\breve{\sigma}}{E}. \tag{126}$$

Since the regularized strain verifies Eq. (115), we can calculate the displacement jump $[\![\breve{u}]\!]$ through the relation

$$[\![\breve{u}]\!] = (\bar{\varepsilon}(x_0) - \varepsilon^{hom})V(x_0). \tag{127}$$

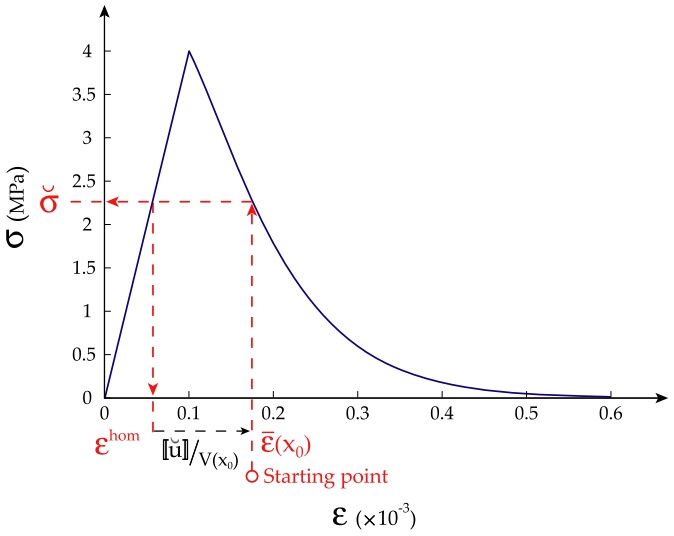

Fig. 18. Method of resolution of the nonlocal problem.

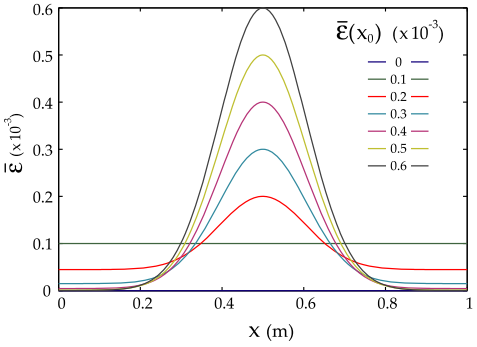

Fig. 19. Resulting regularized strain field as a function of $\bar{\varepsilon}(x_0)$.

The method for obtaining $\breve{\sigma}$, ε^{hom} and $[\![\breve{u}]\!]$ is summarized in diagram 18.

Knowing ε^{hom} and $[\![\breve{u}]\!]$, one can calculate the strain field over the whole length of the beam using relation (114). A spatial discretization of the beam into 1000 segments was chosen for the computations. The plot of Fig. 19 shows the strain curves corresponding to different values of the control variable $\bar{\varepsilon}(x_0)$.

The damage variable field was calculated for that discretization using relation (120). Then, the increment of dissipated energy can be calculated at each time step, which provides the information needed for the calculation of the model with the cohesive zone.

6.5.3. Resolution of the damage problem with the cohesive zone

The resolution of the damage problem with the cohesive zone is carried out using the increments of dissipated energy calculated with the nonlocal model, in a way similar to 6.3. The global resolution of the problem with the different models is summarized in diagram 20.

In Fig. 21(a), we plotted the displacement u_r at the end of the beam and the displacement jump $[\![\hat{u}]\!]$ at the discontinuity as functions of time. This curve also shows the displacement jump $[\![\breve{u}]\!]$ which was used to obtain the analytical solution of the nonlocal model. The fact that the two displacement jump curves are identical shows that the "mechanical" vision and the "energy" vision of model coupling are, for this example, consistent with each other. In Fig. 21(b), the behavior law of the cohesive model $\sigma^s = f([\![\hat{u}]\!])$ is compared to the stress in the damaged beam $\breve{\sigma} = f([\![\hat{u}]\!])$. Again, one can observe that the two curves are identical.

The two curves in Fig. 22 show that the two models are, indeed, equivalent energy-wise, in terms of both dissipated energy and free energy.

7. Toward a generalization to bidimensional and tridimensional cases

The change of model method can be used in bidimensional and tridimensional calculations, at least for straight cracks and mode I decohesion. The determination of the cohesive law increments then requires knowing at each point of the discontinuity the surface energy to be dissipated. As a consequence, the coupling criterion should be defined at each point of the discontinuity instead of being a global criterion. In order to obtain this local criterion, we assume that the position of the crack is known beforehand and we decompose the surrounding of the crack in cylinders perpendicular to the direction of the discontinuity as in Fig. 23.

We consider one cylinder $\mathscr{V}$. The intersection of $\mathscr{V}$ with the crack surface is called $\mathscr{S}$. The half-length l of the cylinder is defined so that $\mathscr{V}$ gets through the whole damaged zone. The coupling criterion 47 is written for this cylinder:

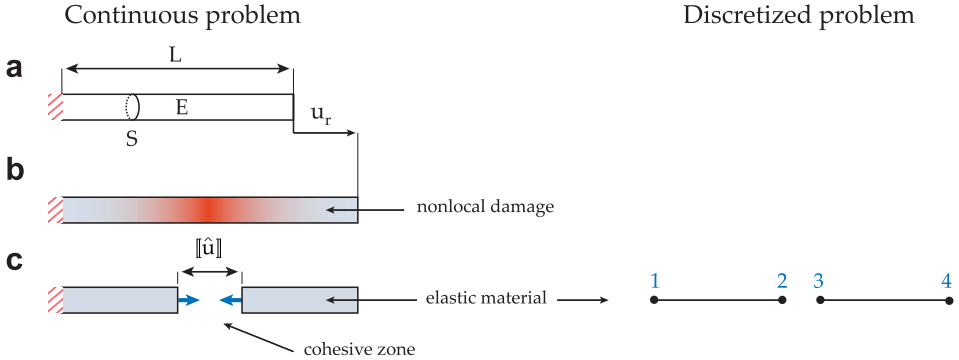

Fig. 20. Resolution of the problem with the two models.

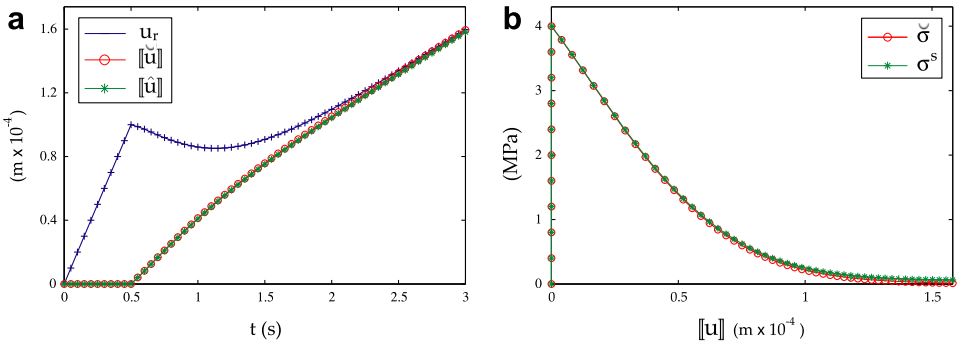

Fig. 21. (a) Displacement at the end of the beam and displacement jump for the cohesive model and (b) traction curve for the cohesive model.

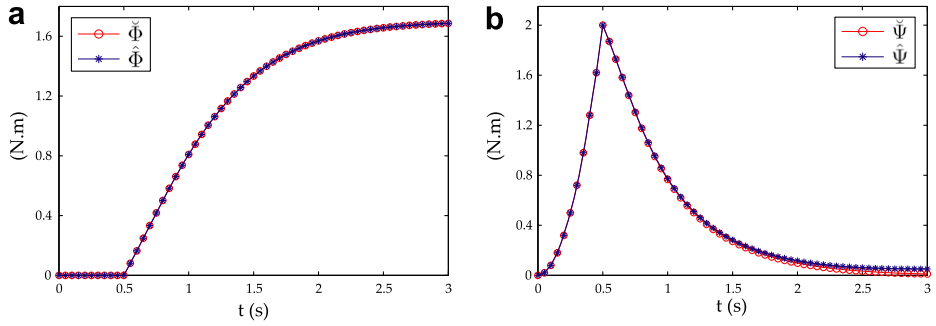

Fig. 22. Verification of the equivalence in terms of dissipated energy (a) and free energy (b).

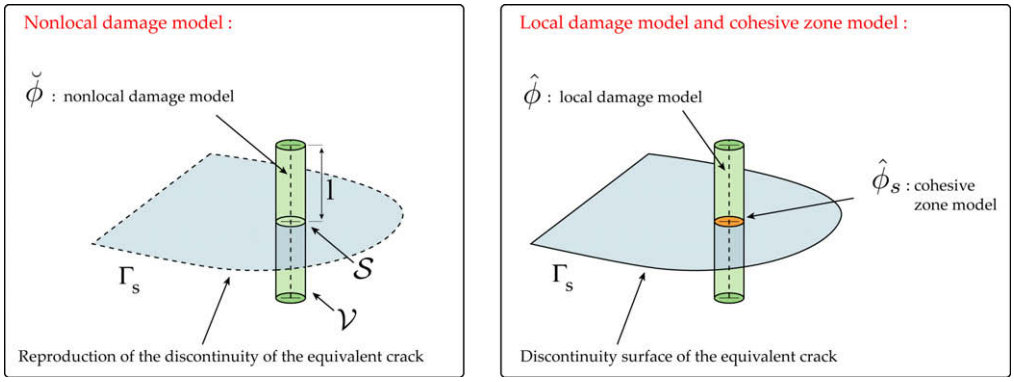

Fig. 23. Cylinders perpendicular to the discontinuity surface.

$$\int_{\mathscr{V}} \breve{\phi}\, dV = \int_{\mathscr{V}} \hat{\phi}\, dV + \int_{\mathscr{S}} \hat{\phi}_s\, dS. \tag{128}$$

By grouping the volume terms we obtain an expression equivalent to (48):

$$\int_{\mathscr{S}} \hat{\phi}_s\, dS = \int_{\mathscr{V}} (\breve{\phi} - \hat{\phi}) dV. \tag{129}$$

The integration over the volume can be decompose in an integration over $\mathscr{S}$ and another over the segment perpendicular to the crack surface, between $-l$ and l, so that

$$\int_{\mathscr{S}} \hat{\phi}_s\, dS = \int_{\mathscr{S}} \left(\int_{-l}^{l} (\breve{\phi} - \hat{\phi}) dl \right) dS. \tag{130}$$

If we consider that the section of the cylinder is small enough so that variables remain stable over a section, the coupling criterion becomes

$$\hat{\phi}_s = \int_{-l}^{l} (\breve{\phi} - \hat{\phi}) dl. \tag{131}$$

We obtain with Eq. (131), a local coupling criterion for each point of the discontinuity. This criterion can be detailed by taking into account the local stability of the damaged zone. We will distinguish for each point of the discontinuity the coupling criterion before and after initiation. The initiation of the cohesive zone will be caused by the loss of stability criterion ($d\underline{\underline{\sigma}} : d\underline{\underline{\varepsilon}} > 0$) when the material enters into the softening part of the behavior law. Before initiation of the crack at a point, the behavior of the material is stable on the corresponding segment so that we can assume that $d\breve{\phi} = d\hat{\phi}$. As a consequence, the coupling criterion is

$$d\hat{\phi}_s = 0 \quad \text{before localization.} \tag{132}$$

After initiation of the crack at a point of the discontinuity, the material surrounding the crack unloads and we can assume that on the

corresponding segment $d\hat{\phi} = 0$. The change of model criterion then writes

$$d\hat{\phi}_s = \int_{-l}^{l} d\breve{\phi}\, dl \quad \text{after localization.} \tag{133}$$

In the one-dimensional case, Eqs. (132) and (133) multiplied by the section S of the beam permit to recover Eqs. (49) and (50).

8. Conclusion

We have presented a method which enables one to couple the two approaches (continuous and discontinuous) to the localized rupture of a material. This coupling is achieved by enforcing equal dissipated energies in the two models. The conservation of the other energy balance terms is guaranteed by using a cohesive model with linear closing which is consistent with the chosen damage elastic model. An important point is to determine when the macroscopic crack is initiated. Since we consider that discontinuous models play the role of localization limiters, the initiation of the discontinuity coincides with the loss of material stability. Thus, the energy dissipated by the nonlocal model is transferred to the cohesive zone only once the material enters the softening part of the traction curve.

This method was used for the calculation of traction curves of cohesive models based on nonlocal (or quasi-nonlocal) damage models. We proposed two methods for calculating the solution of the damage model with a cohesive zone. The first method consists in writing down all the equations of the problem in order to derive a differential equation for the behavior of the cohesive zone. The second method is based on the use of a Lagrange multiplier to enforce the amount of energy dissipated at the discontinuity. The latter method can be used with any nonlocal damage model and in the framework of finite element analysis. One could also use a second-gradient model or a delayed-effect model in place of the nonlocal model.

The method can be used in two steps. First, a calculation is carried out on a simple geometry for the nonlocal model while the coupling criterion enables to get the shape of the equivalent cohesive law. Second, a calculation on a complex structure is performed with the equivalent cohesive zone model and classical local damage model alone. The possible extension of the method to bidimensional and tridimensional cases with straight cracks has been briefly presented. Some further investigations are needed to validate the method for those cases. In particular, one can wonder if the cohesive zone model obtained will be the same at each point of the discontinuity. The method presented herein has been constructed with the assumption that there is no plastic deformation in the material. A possible evolution would be to generalize it so that it can be used with any plastic-damageable reference model.

Acknowledgements

We thank the SAFRAN group for its financial support for this work (Contract YHMMV_2007_012).

References

Aifantis, E., 1984. On the structural origin of certain inelastic models. Journal of Engineering Materials and Technology 106, 326–330.
Barenblatt, G., 1962. The mathematical theory of equilibrium cracks in brittle fracture. Advances in Applied Mechanics 7, 55–129.
Bažant, Z., Belytschko, T., Chang, T., 1984. Continuum theory for strain-softening. Journal of Engineering Mechanics 110 (12), 1666–1692.
Bažant, Z., Oh, B., 1983. Crack band theory for fracture of concrete. Materials and Structures 16 (3), 155–177.
Belytschko, T., Black, T., 1999. Elastic crack growth in finite elements with minimal remeshing. International Journal for Numerical Methods in Engineering 45 (5), 601–620.
Charlotte, M., Francfort, G., Marigo, J.-J., Truskinovsky, L., 2000. Revisiting brittle fracture as an energy minimization problem: comparisons of griffith and barenblatt surface energy models. In: Continuous Damage and Fracture, pp. 7–18.
Charlotte, M., Laverne, J., Marigo, J.-J., 2006. Initiation of cracks with cohesive force models: a variational approach. European Journal of Mechanics-A/Solids 25, 649–669, 6th EUROMECH Solid Mechanics Conference.
Comi, C., Mariani, S., Perego, U., 2002. On the transition from continuum nonlocal damage to quasi-brittle discrete crack models. In: GIMC_2002 Third Joint Conference of Italian Group of Computational Mechanics and Ibero-Latin American Association of Computational Methods in Engineering.
Comi, C., Mariani, S., Perego, U., 2007. An extended FE strategy for transition from continuum damage to mode I cohesive crack propagation. International Journal for Numerical and Analytical Methods in Geomechanics 31 (2), 213–238.
Costanzo, F., Allen, D., 1995. A continuum thermodynamic analysis of cohesive zone models. International Journal of Engineering Science 33 (15), 2197–2219.
Dugdale, D., 1960. Yielding of steel sheets containing slits. Journal of the Mechanics and Physics of Solids 8, 100–108.
Griffith, A., 1920. The phenomena of rupture and flow in solids. Philosophical Transactions of the Royal Society CCXXI (A), 163–198.
Gurtin, M., 1979. Thermodynamics and the cohesive zone in fracture. Zeitschrift für Angewandte Mathematik und Physik (ZAMP) 30 (6), 991–1003.
Hadamard, J., 1903. Leçons sur la propagation des ondes et les équations de l'hydrodynamique. librairie scientifique, Paris.
Hill, R., 1962. Acceleration waves in solids. Journal of the Mechanics and Physics of Solids 10, 1–16.
Hillerborg, A., Modèer, M., Petersson, P., 1976. Analysis of crack formation and crack growth in concrete by means of fracture mechanics and finite elements. Cement and Concrete Research 6, 773–782.
Kachanov, L., 1958. Time of rupture process under creep conditions. Izvestia Akademii Nauk SSSR, Otd. Tekh. Nauk 8, 26–31.
Ladevéze, P., 1992. A damage computational method for composite structures. Computers and Structures 44, 79–87.
Lasry, D., Belytschko, T., 1988. Localization limiters in transient problems. International Journal of solids and Structures 24 (6), 581–597.
Legrain, G., Dufour, F., Huerta, A., Pijaudier-Cabot, G., Barcelona, 2007. Extraction of crack opening from a nonlocal damage field. In: COMPLAS, IX International Conference on Computational Plasticity, Fundamentals and Applications.
Lemaitre, J., Chaboche, J.-L., 1988. Mècanique des matériaux solides. Dunod.
Mariani, S., Perego, U., 2003. Extended finite element method for quasi-brittle fracture. International Journal for Numerical Methods in Engineering 58, 103–126.
Mazars, J., 1984. Application de la mécanique de l'endommagement au comportement non-linéaire et à la rupture du béton de structure. Ph.D. thesis, ENSET.
Mazars, J., Pijaudier-Cabot, G., 1996. From damage to fracture mechanics and conversely: a combined approach. International Journal of Solids and Structures 33 (20–22), 3327–3342.
Moes, N., Dolbow, J., Belytschko, T., 1999. A finite element method for crack growth without remeshing. International Journal for Numerical Methods in Engineering 46 (1), 131–150.
Moës, N., Belytschko, T., 2002. Extended finite element method for cohesive crack growth. Engineering Fracture Mechanics 69, 813–833.
Ortiz, M., Leroy, Y., Needleman, A., 1987. A finite element method for localized failure analysis. Computer Methods in Applied Mechanics and Engineering 61 (2), 189–214.
Peerlings, R., Geers, M., de Borst, R., Brekelmans, W., 2001. A critical comparison of nonlocal and gradient-enhanced softening continua. International Journal of solids and Structures 38, 7723–7746.
Pijaudier-Cabot, G., Bažant, Z., 1987. Nonlocal damage theory. Journal of Engineering Mechanics 113 (10), 1512–1533.
Planas, J., Elices, M., Guinea, G., 1993. Cohesive cracks versus nonlocal models: closing the gap. International Journal of Fracture 63 (2), 173–187.
Rice, J., 1968. A path independent integral and the approximate analysis of strain concentration by notches and cracks. Journal of Applied Mechanics 35, 379–386.
Simo, J., Oliver, J., Armero, F., 1993. An analysis of strong discontinuities induced by strain-softening in rate-independent inelastic solids. Computational Mechanics 12 (5), 277–296.
Simone, A., Wells, G., Sluys, L., 2003. From continuous to discontinuous failure in a gradient-enhanced continuum damage model. Computer Methods in Applied Mechanics and Engineering 192 (41), 4581–4607.
Wells, G., Sluys, L., 2001. A new method for modelling cohesive cracks using finite elements. International Journal for Numerical Methods in Engineering 50, 2667–2682.